Binding Modes of the Precursor of Adenovirus Major Core Protein VII to DNA and Template Activating Factor I: Implication for the Mechanism of Remodeling of the Adenovirus Chromatin†

Béla Gyurcsik,‡,§,|| Hirohito Haruki,‡,§ Tsuyoshi Takahashi,⊥ Hisakazu Mihara,⊥ and Kyosuke Nagata*,§

Department of Infection Biology, Graduate School of Comprehensive Human Sciences, and Institute of Basic Medical Sciences, University of Tsukuba, 1-1-1 Tennodai, Tsukuba 305-8575, Japan, Department of Inorganic and Analytical Chemistry, University of Szeged, Szeged H-6701, Hungary, and Department of Bioengineering, Graduate School of Bioscience and Biotechnology, Tokyo Institute of Technology, 4259 Nagatsuta-cho, Midori-ku, Yokohama 226-8501, Japan

Received June 29, 2005; Revised Manuscript Received November 1, 2005

ABSTRACT: Template Activating Factor (TAF) I remodels the adenovirus (Ad) core structure composed of the Ad genome DNA and basic viral core proteins and stimulates in vitro DNA replication and transcription of the Ad core. We have recently reported that TAF-I binds to major core protein VII and forms DNA−protein VII−TAF-I ternary complexes in vitro and in vivo. Further to understand the mechanism of remodeling of the Ad core, we characterized the interaction mode between the precursor of protein VII (pre-VII) and either DNA or TAF-I by means of biochemical and biophysicochemical methods. We found that a major binding region of pre-VII with both DNA and the acidic carboxyl-terminal region of TAF-I lies in the arginine-rich region of pre-VII. Both amino-terminal and carboxyl-terminal regions of pre-VII without the arginine-rich region directly bound to DNA and supported the DNA binding activity of the arginine-rich region. A TAF-I mutant protein lacking the acidic carboxyl-terminal region bound preferentially to the carboxyl-terminal region of pre-VII containing the arginine-rich region rather than the amino-terminal region of pre-VII. Thus, DNA interacted with the entire region of pre-VII, while TAF-I bound preferentially to the carboxyl-terminal region of pre-VII. This binding mode suggests the formation of the ternary complexes among DNA, protein VII, and TAF-I. On the basis of the binding modes in binary systems, we discussed the remodeling mechanism of the Ad core in early phases of infection.

Compaction of the eukaryotic genome DNA is mediated by its tight interaction with basic proteins such as histones and sperm-specific basic proteins in somatic and sperm nuclei, respectively. Chromatin regulation factors are involved in remodeling and maintenance of the nucleoprotein complex structure and regulation of events related to DNA. Such factors are categorized into three families, histone-modifying enzymes (*1*), multisubunit ATP-dependent chromatin remodeling factors (*2*), and histone chaperones (*3*). Histone chaperones bind to histones and dissociate and deposit histones from and to DNA, respectively. Rapid and global decondensation of sperm chromatin of invertebrates and some vertebrates is mediated through removal of sperm-specific basic proteins from sperm chromatin by direct interaction with histone chaperones such as nucleoplasmin and TAF-I (*4*−*6*) immediately after fertilization.

Adenovirus (Ad)[1] contains the double-stranded DNA genome, which is condensed and forms the Ad core structure with virus-encoded basic core proteins V and VII and polypeptide X (*7*). In Ad-infected cells, DNA complexed with core protein VII functions as template for early gene transcription and presumably the first round of replication of the Ad DNA (*8*−*10*). By dissecting and reconstituting in vitro systems of replication and transcription using the Ad core as template, we have identified host factors designated Template Activating Factor (TAF) I/SET (*11*−*14*), TAF-II/NAP-1 (*15*), and TAF-III/nucleophosmin/B23 (*16*). These remodel the Ad core and stimulate replication and transcription of the Ad genome DNA in vitro. TAF-I, TAF-II, and TAF-III contain one or more of the characteristic acidic cluster composed of aspartic acid and glutamic acid. All three proteins possess both histone chaperone activity and decondensation activity of *Xenopus* sperm nuclei (*6*, *17*).

† This work was supported in part by a grant-in-aid from the Ministry of Education, Culture, Sports, Science, and Technology and by grants from the Bioarchitect Reserch Program from RIKEN and the Mitsubishi Foundation (to K.N.). B.G., on leave from University of Szeged, was supported by a one-year fellowship in the frame of the 36th UNESCO International Course for Advanced Research in Chemistry and Chemical Engineering.

* To whom correspondence should be addressed. Phone/Fax: (81) +29-853-3233. E-mail: knagata@md.tsukuba.ac.jp.

‡ The first and second authors of this papar equally contributed to this work.

§ University of Tsukuba.

|| University of Szeged.

⊥ Tokyo Institute of Technology.

[1] Abbreviations: TAF, template activating factor; Ad, adenovirus; pre-VII, precursor of protein VII; RRR, arginine-rich region; CBB, Coomassie Brilliant Blue; PAGE, polyacrylamide gel electrophoresis; aa, amino acid(s); His, hexahistidine.

10.1021/bi051248+ CCC: $33.50
Published on Web 12/07/2005

Recently, we showed that TAF-I binds to core protein VII and facilitates to form nuclease-accessible ternary nucleoprotein complexes in vitro (*18*). The ternary complex is also found in early phases of infection (*18*). TAF-I consists of a homo- or heterodimer between TAF-Iα and TAF-I*β* through the coiled-coil structure common to both proteins (*19*). TAF-Iα and TAF-I*β* differ only at the short amino-terminal region. The characteristic structure of TAF-I is a highly acidic cluster of ~55 amino acids (aa) at its carboxyl-terminal region, designated "acidic tail". Both the acidic tail and dimerization through the coiled-coil structure are required for remodeling of the Ad core (*13*, *19*). On the other hand, protein VII is a highly basic arginine-rich DNA binding protein (*8*, *20*, *21*). Protein VII is synthesized as a precursor of protein VII (pre-VII) in late phases of infection (*22*). The 24 aa precursor portion at the amino-terminal region is highly conserved among different Ad species (*23*). It is cleaved by Ad-encoded protease at the final stage of virion maturation (*22*). Pre-VII of human Ad type 2 and type 5 contains the highly arginine-rich region (RRR) of about 20 aa in the middle region, which has significant similarity with an arginine cluster of a protamine, one of sperm basic proteins. In addition to RRR, both amino-terminal and carboxyl-terminal regions are also basic, p*I* values of which are about 10.5 and 12.5, respectively. DNA−protein VII complexes once formed are extremely stable (*20*). DNA binding sites of protein VII and pre-VII in virus particles are roughly mapped with protease digestion and UV light-induced cross-linking assays (*24*, *25*). It is suggested that RRR binds to the phosphate backbone of DNA, while α-helices in the carboxyl-terminal portion of protein VII dock with the major groove of DNA (*25*).

In this report, to gain better insight into the mechanism of remodeling of the Ad nucleoprotein complexes by TAF-I, we studied the binding mode between pre-VII and either DNA or TAF-I. We found that TAF-I interacts with pre-VII in late phases of infection and protein VII in early phases of infection. We determined binding regions in binary systems either between pre-VII and DNA or between pre-VII and TAF-I using recombinant pre-VII and TAF-I proteins including their mutant proteins. The interaction mode was analyzed by means of nitrocellulose filter binding, fluorescence anisotropy, pull-down, and protease sensitivity assays. We found that the major binding region of pre-VII with both DNA and TAF-I contains RRR of pre-VII. RRR strongly interacts with the negatively charged DNA and the acidic tail of TAF-I. Both amino-terminal and carboxyl-terminal regions of pre-VII supported DNA binding of pre-VII by their direct interaction with DNA. We showed that a TAF-I mutant protein lacking the acidic tail binds to the carboxyl-terminal region of pre-VII containing RRR. Thus, DNA interacts with the entire region of pre-VII, while TAF-I binds to the carboxyl-terminal region and RRR of pre-VII. This binding mode in binary systems is discussed in relation with the possible mechanism of remodeling of the Ad DNA−protein VII complex in early phases of infection.

EXPERIMENTAL PROCEDURES

Co-immunoprecipitation Assay. HeLa cells were infected with CsCl-purified human Ad type 5 at the multiplicity of infection of 20. At indicated time points postinfection, cells were washed with phosphate-buffered saline and collected in test tubes. Cells [$(1-2) \times 10^7$] were suspended in a lysis buffer (10 mM Tris-HCl, pH 7.9, 50 mM NaCl, 1 mM EDTA, 0.1% BSA, and 0.5% NP40) and disrupted by sonication. After sonicated extracts were clarified by centrifugation, supernatant fractions were incubated with rat anti-protein VII antibody (*18*) or mouse anti-TAF-I*β* antibody (KM1721) (*26*). Then, protein A−Sepharose beads (Amersham Bioscience) were added. After incubation for 1 h, the beads were washed twice with the lysis buffer without BSA and boiled in an SDS sample buffer (60 mM Tris-HCl, pH 6.8, 10% glycerol, and 2% SDS). Proteins were separated by 12.5% SDS−PAGE and immunoblotted with either anti-TAF-I*β* antibody or anti-protein VII antibody.

Preparation of the Proteins. Hexahistidine- (His-) tagged TAF-I*β*, TAF-I*β*ΔC (lacking the acidic carboxyl-terminal region), and TAF-I*β*PME (containing point mutations in the coiled-coil region to prevent dimer formation) were prepared as previously described (*13*, *19*). Recombinant His-pre-VII and protein VII were prepared as described (*18*). For preparation of recombinant pre-VII without the His tag, we utilized the Glu-C digestion site of His-pre-VII located just one amino acid before the first methionine of pre-VII [-G-S-H-M-L-E (Glu-C digestion)-M (first methionine of pre-VII)-S-I-L-I-]. His tag was removed by partial digestion of His-pre-VII with Glu-C (Promega). Briefly, His-pre-VII (150 ng/μL) was incubated at 37 °C for 1 h with Glu-C (0.025 ng/μL) in 50 mM ammonium bicarbonate. After addition of $^1/_{50}$ volume of 0.5 M diisopropyl fluorophosphates in 2-propanol, final concentrations of Tris-HCl, pH 7.9, urea, and NaCl were adjusted to 20 mM, 6 M, and 0.2 M, respectively. The mixture was loaded on an Uno-S column (Bio-Rad), and pre-VII was eluted with 30 mL of a linear gradient of 0.5−1.5 M NaCl in buffer A (20 mM Tris-HCl, pH 7.9, and 6 M urea). His-pre-VII deletion mutant proteins were prepared as follows: DNA fragments corresponding to pre-VII(1−92) (numbers indicate aa positions, where the amino-terminal aa of pre-VII is designated as 1), pre-VII-(1−115), and the amino-terminal region of pre-VII(Δ93−115) were amplified by PCR using plasmid pET14b-pre-VII (*18*) as template and a set of primers, a common amino-terminal primer, 5′-GCCTCGAGATGTCCATCCTTATATC-GCCC-3′, and one of primers 5′-CGGGATCCCTAGGCTC-CGCGCACCACGG-3′, 5′-CGGGATCCCTAAGTGCCGG-GTCGGCGGC-3′, and 5′-CGCGCGTTGGGCGGCGGCT-CCGCGCACCACGG-3′, respectively. DNA fragments corresponding to pre-VII(93−198), pre-VII(116−198), and the carboxyl-terminal region of pre-VII(Δ93−115) were amplified by PCR using pET14b-pre-VII as template and using a set of primers, a common T7 terminator primer, 5′-GCTAGTTATTGCTCAGCGG-3′, and one of primers 5′-GCCTCGAGCGGCGCTATGCTAAAATGAAGAG-3′, 5′-GCCTCGAGGCCGCCCAACGCGCG-3′, and 5′-GCC-GCCCAACGCGCG-3′, respectively. A DNA fragment corresponding to the full-sized pre-VII(Δ93−115) was prepared by overlapping PCR using DNA fragments of amino- and carboxyl-terminal regions of pre-VII(Δ93−115), the common amino-terminal primer, and the common T7 terminator primer. The resultant DNA fragments were digested with *Xho*I [pre-VII(1−198), pre-VII(Δ93−115), pre-VII(93−198), and pre-VII(116−198) fragments] and *Xho*I and *Bam*HI [pre-VII(1−92) and pre-VII(1−115) fragments] and cloned into the *Xho*I and *Xho*I/*Bam*HI digested pET14b, respectively. Sequences were confirmed by the dideoxy sequencing

method. Proteins were expressed in bacteria and purified by Ni^{2+} affinity chromatography as described (*18*). Affinity-purified proteins were loaded on an Uno-S column and eluted with 30 mL of a linear gradient of 0.2−1 M NaCl in buffer A. Peak fractions were collected and dialyzed against water. The protein concentration was calculated from absorbance of proteins at 280 nm using its estimated extinction coefficient (*27*).

Solid-Phase Synthesis of the Short Peptides. Fmoc-Gly-OH, Fmoc-Glu(OtBu)-OH, Fmoc-Asp(OtBu)-OH, and Fmoc-Met-OH were used for TAF-Iβ(224−244), NH_2-DMDDEEGEGEEDDDDDEEEEG-$CONH_2$. Peptide synthesis was initiated on 0.06 mmol of Rink amide resin [4-(2′,4′-dimethoxyphenyl-Fmoc-aminomethyl)phenoxy resin]. Reactions were carried out in 1-methyl-2-pyrrolidone (NMP) in a batch form under a manual control. Cleavage of Fmoc was performed by 20% piperidine in NMP. After repeated washes with NMP, amino acid coupling was performed using a 3-fold molar excess of an appropriate Fmoc-amino acid dissolved in NMP to the resin. A 3-fold molar excess of 2-(1*H*-benzotriazol-1-yl)-1,1,3,3-tetramethyluronium hexafluorophosphate and *N*-hydroxybenzotriazole hydrate was added to this solution. A 6-fold molar excess of diisopropylethylamine was added immediately before the solution was loaded onto the resin. The coupling reaction was performed for 15−30 min followed by the Kaiser test (*28*) after each coupling step. After the final deprotection step, the resin was washed by NMP and chloroform and dried under vacuum. The cleavage of the peptide from the resin was performed at room temperature for 1 h with slow stirring of the slurry in the mixture of 10 mL of trifluoroacetic acid, 0.25 mL of *m*-cresol, 0.75 mL of ethanedithiol, and 0.75 mL of thioanisole. After filtering, the peptide was precipitated and washed by diethyl ether. The crude peptides were purified with reverse-phase HPLC on a ODS A-323 column (10 × 250 mm) (YMC) using a linear gradient of 5−40% acetonitrile/0.1% trifluoroacetic acid. The fluorescent probe-labeled peptides with 5- (and 6-) carboxyfluorescein succinimidyl ester [5(6)-FAM SE] fluorescent probe attached to their amino termini were prepared by the same method as above. The product was identified by reverse-phase HPLC and MALDI-TOF-MS.

Pull-Down Assays. His-TAF-Iβ, His-TAF-IβPME, and His-TAF-I$\beta\Delta$C were immobilized on protein A−Sepharose beads by incubating with anti-TAF-Iβ antibody (KM1721) and each TAF-I mutant protein in IP buffer (40 mM Tris-HCl, pH 7.9, 0.5 mg/mL BSA, and 0.5% NP-40) containing 150 mM NaCl. Then, beads were washed extensively with IP buffer. The amount of each TAF-I protein immobilized on the beads was estimated by SDS−PAGE followed by staining with Coomassie Brilliant Blue (CBB). Each TAF-I mutant protein (250 ng) immobilized on the beads was incubated at 4 °C for 1.5 h with the indicated amount of pre-VII or its mutant proteins in 0.5 mL of IP buffer containing 150, 300, or 500 mM NaCl with constant rotating. Then, the beads were washed twice with the same buffer and once with IP buffer containing 150 mM NaCl without BSA and boiled at 98 °C for 2 min in the SDS sample buffer. Proteins were separated by 12.5% SDS−PAGE and visualized with CBB staining.

Filter Binding Assays. Radiolabeled DNA was prepared by digestion of pUC119 plasmid DNA with *Msp*I followed by endo labeling with Klenow fragment in the presence of [α-^{32}P]dCTP. DNA (25 μL) in a 2 × binding buffer (50 mM Tris-HCl, pH 7.9, and various concentrations of NaCl) containing 10 ng of radiolabeled dsDNA (10000−20000 counts/min) and 200 ng/mL BSA was mixed with 25 μL of a pre-VII mutant protein in water. The reaction mixture was incubated at room temperature for 30 min and filtered through a nitrocellulose membrane (Hybond ECL; Amersham Bioscience) that had been soaked in the binding buffer. The filter was washed once with 0.4 mL of the binding buffer. The filter was cut in pieces, and the radioactivity was counted by Cerenkov radiation.

Fluorescence Anisotropy Measurements. All spectroscopic measurements were carried out at 25 °C in a solution containing 20 mM Tris-HCl, pH 7.4, and 150 mM NaCl. The fluorescence measurement was performed with a RF-5300PC fluorescence spectrophotometer (Shimadzu) using a 1 cm path-length quartz cell. Fluorescence anisotropy was calculated by the intensities at 520 nm excited at 490 nm using the equation:

$$A = \frac{I_{0°,0°} - I_{0°,90°}G}{I_{0°,0°} + 2I_{0°,90°}G}$$

where $G = I_{90°,0°}/I_{90°,90°}$ and $I_{i,j}$ indicates the fluorescence intensity when the excitation side and the emission side polarizers are set at i and j degrees, respectively, while G stands for the polarization characteristics of the instrument.

Protease Sensitivity Assays. His-pre-VII (1.2 μg, 49 pmol) was incubated at 37 °C for 15 min in the absence or presence of the equal amount of plasmid DNA (1 μg) or a 2-fold molar excess of TAF-I (3 μg, 93 pmol) to allow complex formation in 14 μL of digestion buffer (10 mM Tris-HCl, pH 7.9, and 150 mM NaCl). One microliter (1 ng/μL) of α-chymotrypsin (Sigma) was added, and the mixture was further incubated for 5 min. The digestion was stopped by adding 5 μL of 4 × SDS sample buffer. The proteins were boiled at 98 °C for 2 min, separated by 15% SDS−PAGE, and visualized with CBB staining. Identification of the peptide fragments in Figure 7 was performed as follows. His-pre-VII partially digested with chymotrypsin was subjected to MALDI-MS. By comparison with predicted digestion sites of pre-VII with α-chymotrypsin, molecular masses of the digested peptides corresponded to those of aa 14−198, aa 41− and 45−198, aa −22−124 or −137, aa 96− and 99−198, and aa −22−95 and −98 of pre-VII (where the region between aa positions −22 and −1 is derived from the His tag).

RESULTS

Interaction of TAF-I with Pre-VII in Late Phases of Infection. The infecting Ad DNA in the nucleus remains associated with protein VII in early phases of infection. In late phases of infection, pre-VII is synthesized and accumulates in the nucleus to assemble progeny virions. We have shown that TAF-I binds to a DNA−protein VII complex and forms a ternary structure among DNA, protein VII, and TAF-I in early phases of infection (*18*). Immunoprecipitation assays using extracts prepared from cells in early phases of infection showed that TAF-I interacts with protein VII (unpublished observations). It is possible that TAF-I interacts with pre-VII in late phases of infection. To

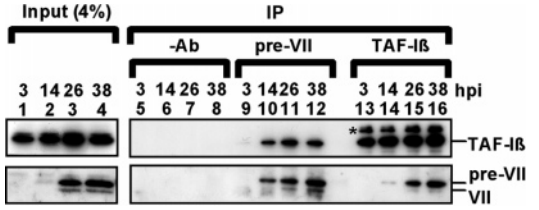

FIGURE 1: Co-immunoprecipitation analysis. HeLa cells were infected with human Ad type 5 at a multiplicity of infection of 20 and collected at indicated times postinfection. Extracts were prepared and subjected to immunoprecipitation assays with control antibody (lanes 5−8), anti-protein VII antibody (lanes 9−12), and anti-TAF-Iβ antibody (lanes 13−16). Input (4%, lanes 1−4) and immunoprecipitated (IP) proteins were separated by 12.5% SDS−PAGE and immunoblotted with anti-TAF-Iβ antibody (upper panels) and anti-protein VII antibody (lower panels). The asterisk indicates the bands derived from the heavy chain of immunoglobulin G of the anti-TAF-Iβ antibody.

examine the interaction between TAF-I and pre-VII, we performed immunoprecipitation assays (Figure 1). HeLa cells were infected with human Ad type 5 at the multiplicity of infection of 20 and collected at indicated time points postinfection as shown in Figure 1. Western blot analyses of these extracts with anti-protein VII antibody revealed that pre-VII begins to accumulate as early as 14 h postinfection (lane 2), and protein VII appears at 26 h postinfection (lane 3). Incoming protein VII was not detected because its amount was below the detection limit by western blotting. Immunoprecipitation assays using these extracts showed that TAF-I is coprecipitated with pre-VII (lanes 9−12) and pre-VII is coprecipitated with TAF-I (lanes 13−16). These results indicate that TAF-I interacts with pre-VII in late phases of infection as well as with protein VII in early phases of infection (unpublished observations). Thus, it is assumed that TAF-I plays a role(s) during late phases of infection. To understand the binding property of pre-VII−TAF-I complexes compared with that of protein VII−TAF-I complexes (*18*), we performed biochemical analyses hereafter focusing on the interaction of pre-VII with either DNA or TAF-I.

Regions of Pre-VII Responsible for Binding with DNA. To identify a DNA binding region(s) of pre-VII, we carried out filter binding assays using recombinant pre-VII proteins including various deletion mutant proteins (Figures 2 and 3). First, we tried to compare the DNA binding activity of protein VII with that of pre-VII. Simultaneously, we examined the DNA binding activity of pre-VII compared with that of His-pre-VII to see whether it is appropriate to use His-tagged proteins for convenience. All proteins generated in bacteria were purified to the apparent homogeneity (Figure 2B). The DNA binding activity of His-pre-VII, pre-VII, and protein VII was examined by the filter binding assay in the presence of 150 and 300 mM NaCl (Figure 3A). All of these proteins bound to DNA with similar affinity under both conditions. Since the difference of DNA binding activity, if any, was a little among three proteins, we designed deletion mutant proteins based on pre-VII containing a His tag (Figure 2A). Pre-VII contains a highly positively charged region between amino acid (aa) positions 95 and 113. We designated this region as arginine-rich region (RRR). RRR is one of the candidate regions involved in binding to the negatively charged molecules such as DNA and TAF-I. Pre-VII deletion mutant proteins were prepared as shown in Figure 2. Filter binding assays showed that in a buffer

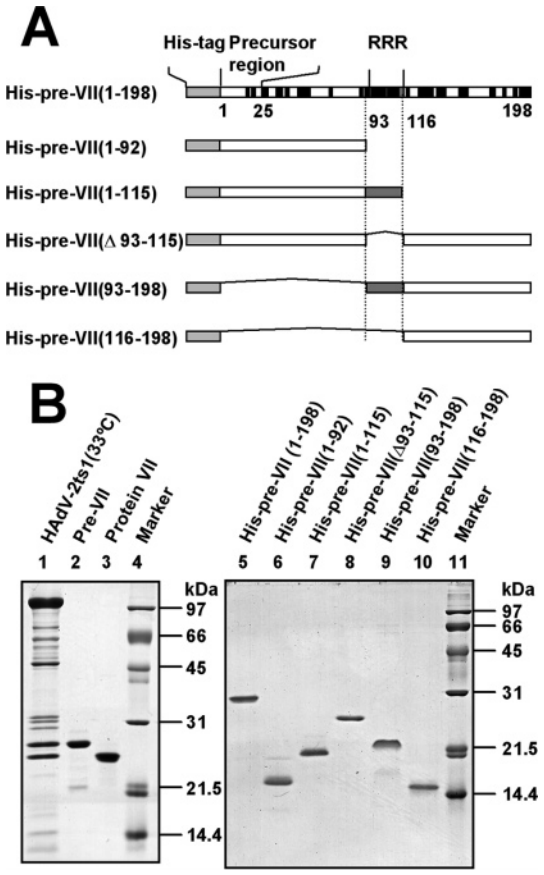

FIGURE 2: Pre-VII mutant proteins used in this study. (A) Schematic representation of pre-VII and its mutant proteins. The sites of arginine and lysine are indicated by the vertical bar on the schematic diagram of His-pre-VII(1−198). His-pre-VII(1−92) is the amino-terminal fragment that does not contain RRR and the carboxyl-terminal region. His-pre-VII(1−115) contains the amino-terminal region and RRR (dark shaded rectangle) but not the carboxyl-terminal region. His-pre-VII(Δ93−115) lacks RRR. His-pre-VII-(93−198) lacks the amino-terminal region. His-pre-VII(116−198) does not contain the amino-terminal region and RRR. (B) Purified recombinant proteins. Proteins were separated by 15% SDS−PAGE and visualized by staining with CBB: lane 1, CsCl-purified virus particles prepared from human Ad type 2 ts1 infected cells maintained at 33 °C (*22*); lanes 2, 3, and 5−10, recombinant proteins.

containing 50 mM NaCl (Figure 3B, upper panel) all deletion mutant proteins bound to DNA but with less binding efficiency than the full-length pre-VII. A pre-VII deletion mutant protein lacking only RRR bound to DNA to a similar extent as mutant proteins lacking either one of the amino-terminal region or the carboxyl-terminal region. These results suggest that amino-terminal and carboxyl-terminal regions as well as RRR possess the DNA binding activity. In fact, the amino-terminal region or the carboxyl-terminal region itself bound to DNA (shown by closed symbols), although the binding efficiency was much less than proteins consisting of both regions. In the presence of 150 mM NaCl (middle panel), the DNA binding activity of the pre-VII mutant proteins consisting of only either the amino-terminal region or the carboxyl-terminal region was completely abolished. The DNA binding activity of pre-VII(Δ93−115) was significantly less than that of the other two proteins lacking only one region of pre-VII. Therefore, we assumed that amino-terminal and carboxyl-terminal regions would increase the DNA binding activity of RRR. In the presence of 300

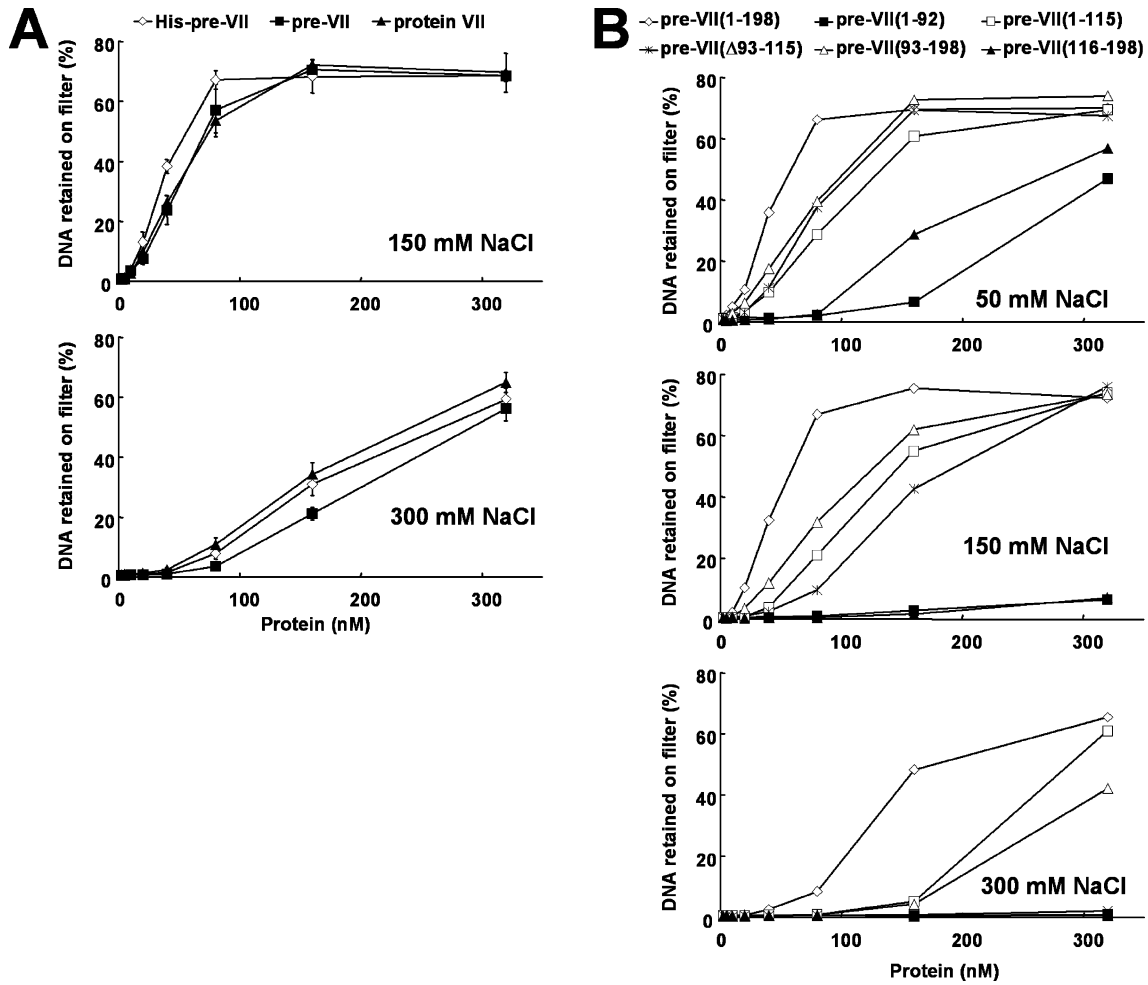

FIGURE 3: DNA binding activity of His-pre-VII mutant proteins. (A) Filter binding assays with protein VII, pre-VII, and His-pre-VII. The reaction mixture (50 μL) containing 10 ng of radiolabeled *Msp*I-digested pUC119 plasmid DNA, 100 ng/μL BSA, 150 or 300 mM NaCl, and increasing amounts of proteins was incubated at room temperature for 30 min. The mixture was filtered through a nitrocellulose membrane and washed once with a buffer containing 25 mM Tris-HCl, pH 7.9, and 150 or 300 mM NaCl. The radioactivity retained on the filter was determined by Cerenkov counting. Results with triplicate assays are indicated with bars of SD. Note that approximately 20% of DNA was lost due to the nonspecific binding of protein VII−DNA complexes to test tubes and others. (B) Filter binding assays using pre-VII mutant proteins. Filter binding assays were performed as described above using His-pre-VII deletion mutant proteins in the presence of the indicated concentrations of NaCl. The average of duplicate assays is indicated.

mM NaCl (lower panel), amino-terminal and carboxyl-terminal regions equipped with RRR bound to DNA but with less efficiency than the full-length pre-VII, while pre-VII-(Δ93−115) completely lost the DNA binding activity. These results suggest that a major DNA binding region is RRR, and amino-terminal and carboxyl-terminal regions, each of which has the potential DNA binding activity, enhance the DNA binding activity of pre-VII.

Binding Stoichiometry between Pre-VII and TAF-I. In the previous report, we showed by stoichiometry analyses of the protein VII−TAF-I complex that one dimer of TAF-I binds to one protein VII in the presence of excess amounts of TAF-I, and two protein VII molecules bind to one dimer of TAF-I when these proteins are mixed at an equimolar ratio (*18*). To compare the binding stoichiometry between TAF-I and pre-VII to that between TAF-I and protein VII, we performed native PAGE assays to detect His-TAF-I−protein VII complexes and His-TAF-I−pre-VII complexes (Figure 4A). The assays were performed in the presence of 150 mM NaCl. Pre-VII formed stoichiometric complexes with His-TAF-I (complex A) in a similar manner with protein VII when either pre-VII or protein VII was mixed with TAF-I dimer at a ratio of 0.5:1, 1:1, and 1:2 (lanes 2−4 and lanes 6−8). The band of complex B containing pre-VII was obscure in terms of its composition. In the presence of more basic proteins above this level, proteins were aggregated and did not enter a polyacrylamide gel (lanes 5 and 9) as previously described (*18*). To confirm the stoichiometry of the complex of either TAF-I and protein VII or TAF-I and pre-VII, we performed native PAGE assays with a TAF-Iβ monomer mutant, His-TAF-IβPME (*19*). His-TAF-IβPME migrated much faster than His-TAF-I (lane 10). When His-TAF-IβPME was mixed with either protein VII or pre-VII at a molar ratio of 1:1, a complex with mobility similar to that of complex A was dominant (lanes 13 and 17). This result suggests that one TAF-I monomer mutant binds to one protein VII or one pre-VII. However, we could not exclude the possibility that two TAF-I monomer mutants bind to one protein VII or one pre-VII, since the band containing the complex of His-TAF-IβPME and either protein VII or pre-VII has mobility similar to that of complex A (TAF-I:basic protein = 2:1). To address this point, complexes cross-linked with glutaraldehyde were examined through SDS−PAGE (Figure 4B). Mock-treated His-TAF-I and His-TAF-IβPME migrated as a band with

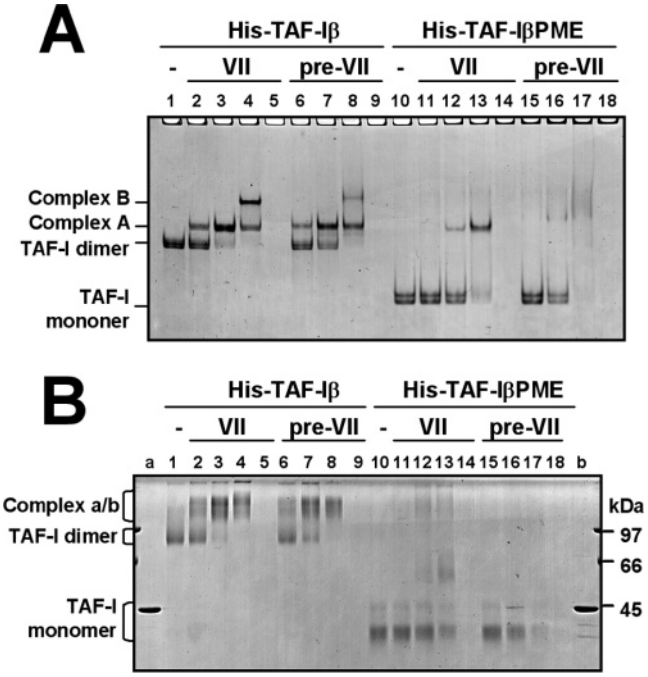

FIGURE 4: Stoichiometry of TAF-I−pre-VII binary complexes. (A) Native PAGE analysis. His-TAF-Iβ (0.5 μg) (lanes 1−9) or His-TAF-IβPME (0.5 μg) (lanes 10−18) was incubated with protein VII ($^1/_4$-, $^1/_2$-, 1-, and 2-fold molar ratio to TAF-I for lanes 2−5 or 11−14, respectively) or pre-VII ($^1/_4$-, $^1/_2$-, 1-, and 2-fold molar ratio to TAF-I for lanes 6−9 or 15−18, respectively) in a buffer containing 5 mM Hepes−NaOH, pH 7.9, 150 mM NaCl, and 10% glycerol. The samples were subjected to separation on a 7.5% polyacrylamide gel in 0.5 × TBE buffer and CBB staining. (B) Cross-linking assay. The same aliquots as in (A) were cross-linked with 0.05% glutaraldehyde at 37 °C for 10 min. The cross-linking reaction was stopped by the addition of the SDS sample buffer. The proteins were separated by 10% SDS−PAGE and visualized by staining with CBB. Lanes a and b indicate native His-TAF-Iβ and His-TAF-IβPME, respectively.

the molecular mass of 45 kDa (lanes a and b). Cross-linked His-TAF-I was shown to have a molecular mass of 80 kDa (lane 1), while cross-linked His-TAF-IβPME migrated faster than the band with a molecular mass of 45 kDa as previously reported (*19*) (lane 10). When the aliquot rich in complex A (Figure 4A, lanes 3 and 7) was subjected to cross-linking, the band with a molecular mass of ∼110 kDa became dominant in a denatured SDS−polyacrylamide gel (Figure 4B, lanes 3 and 7). This result confirmed the formation of a complex consisting of one TAF-I dimer and one protein VII or one pre-VII as previously reported (*18*). From the aliquot rich in His-TAF-IβPME−protein VII complexes (Figure 4A, lane 13), the band with a molecular mass of ∼60 kDa appeared (Figure 4B, lane 13), suggesting the formation of a complex consisting of one TAF-IβPME and one protein VII. From these experiments, we concluded that the binding stoichiometry of the TAF-I−protein VII complex is the same as that of the TAF-I−pre-VII complex: that is, one TAF-I dimer binds to one pre-VII (complex A) and possibly two pre-VIIs (complex B).

Effect of Dimerization and the Acidic Tail of TAF-I on Binding of TAF-I with Pre-VII and Protein VII. Next, we tried to compare the TAF-I binding activity among protein VII, His-tagged pre-VII, and pre-VII without the tag by pull-down assays. Pull-down assays were performed in the presence of 500 mM NaCl using His-TAF-Iβ-immobilized beads (250 ng of TAF-I) as described in Experimental Procedures. When the amount of input basic proteins was less than 400 ng (i.e., during initial binding phases), all three proteins bound to TAF-I with similar efficiency (Figure 5A). His-pre-VII bound more efficiently to TAF-Iβ-bound beads than pre-VII, when the amount of input basic proteins was more than 400 ng (data not shown). It is possible that the His tag of His-pre-VII tends to oligomerize at higher concentrations as previously reported (*29*, *30*). Next, to determine a binding region(s) of TAF-I that is responsible for binding with pre-VII and protein VII, pull-down assays were performed in the presence of 500 mM NaCl using TAF-IβPME mutant- and TAF-I$\beta\Delta$C mutant-bound beads in addition to full-length TAF-Iβ-bound beads (Figure 5C). Neither TAF-IβPME, a dimerization-deficient mutant, nor TAF-I$\beta\Delta$C, an acidic tail deletion mutant (Figure 5B), can remodel the Ad core (*13*, *19*). The amount of input basic proteins used in this assay was set to 200 ng, where the full-length TAF-I bound to pre-VII and protein VII within the linear range as shown in Figure 5A. The upper panel of Figure 5C shows one of the typical results used for quantitative measurement, and the lower panel of Figure 5C is the summary of the repeated experiments. The amount of TAF-I monomer mutant bound to pre-VII or protein VII was about 2-fold less than that of the full-length TAF-I. This result suggests that dimerization of TAF-I is not essential for binding of TAF-I with pre-VII or protein VII but is required for the maximal binding activity. The deletion of the acidic tail from TAF-I had only a small effect on binding of TAF-I with pre-VII or protein VII.

The Amino-Terminal Region of TAF-I without the Acidic Tail Binds to the Carboxyl-Terminal Region of Pre-VII Containing RRR. To more precisely determine the TAF-I binding region of pre-VII, pull-down assays were performed using pre-VII deletion mutant proteins by essentially the same method used for Figure 5C (Figure 6, the upper three panels). The lower panels of Figure 6 show the summary of the binding efficiency of pre-VII mutant proteins to each TAF-I protein. Among the five pre-VII deletion mutants, only His-pre-VII(93−198) in addition to the full-length His-pre-VII-(1−198) bound to the full-length TAF-Iβ even in the presence of 500 mM NaCl, indicating that His-pre-VII(93−198) contains a major TAF-Iβ binding region. Under the same ionic condition, TAF-I monomer mutant and TAF-I mutant lacking the acidic tail were also capable of binding to His-pre-VII(93−198), indicating that the acidic tail and dimerization of TAF-I are not essential for binding of TAF-I to His-pre-VII(93−198) as well as the full-length pre-VII in the presence of 500 mM NaCl. The amount of TAF-IβPME bound to His-pre-VII(93−198) was less compared with the full-length pre-VII. The binding efficiency of TAF-I$\beta\Delta$C to His-pre-VII(93−198) was a little higher than that to the full-length pre-VII. A reason for this result is not known at present. The pre-VII mutant proteins lacking either the carboxyl-terminal region or RRR did not interact with TAF-I in the presence of 500 mM NaCl, suggesting that both the carboxyl-terminal region and RRR are important for binding to TAF-I. In the presence of 300 mM NaCl, in addition to His-pre-VII(1−198) and His-pre-VII(93−198) (data not shown), His-pre-VII(1−115) and His-pre-VII-(Δ93−115) bound to TAF-I (the middle summary panel), suggesting that at lower ionic strength the amino-terminal

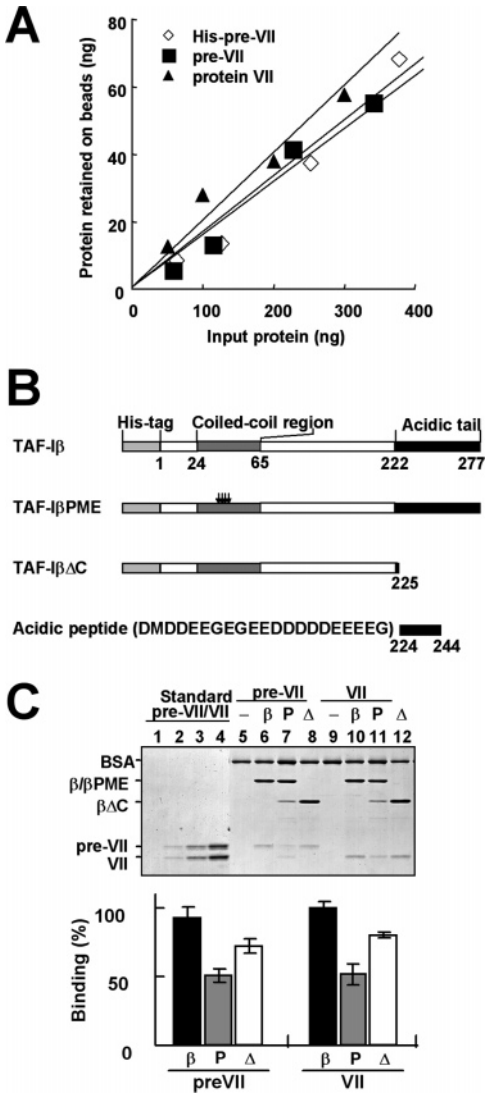

FIGURE 5: TAF-I binding activity to pre-VII and protein VII. (A) Pull-down assays with protein VII, pre-VII, and His-pre-VII. Indicated amounts of input proteins were incubated with His-TAF-Iβ (250 ng) bound beads in a buffer containing 40 mM Tris-HCl, pH 7.9, 0.5 mg/mL BSA, 0.5% NP-40, and 500 mM NaCl. After extensive washing of the beads, proteins retained on the beads and quantitative standards of both pre-VII and protein VII were separated by 12.5% SDS−PAGE and visualized by staining with CBB. The intensity of the bands of each protein was quantified by NIH image. The quantitative standard was used for conversion from the intensity of the bands to the amount (ng) of bound proteins. The average of duplicate assays is indicated. (B) Schematic representation of the TAF-Iβ mutant proteins. TAF-I$\beta\Delta$C lacks the acidic tail, while TAF-IβPME contains four amino acid substitution mutations in the dimerization domain. The acidic peptide, designated TAF-Iβ(224−244), is a part of the acidic tail. (C) Pull-down assays using TAF-I mutant proteins. Pre-VII (228 ng) (lanes 5−8) or protein VII (200 ng) (lanes 9−12) was incubated with His-TAF-I-, His-TAF-I$\beta\Delta$C-, and His-TAF-IβPME-bound beads (250 ng of each TAF-I mutant protein on beads). Proteins retained on the beads and quantitative standards (lanes 1−4) were separated by 12.5% SDS−PAGE and visualized by staining with CBB (upper panel). The amount of proteins bound to beads was quantified as described in (A). Then, the molar ratios of basic protein to acidic protein on the beads were calculated. The maximum value was set to 100%. The value of protein VII and pre-VII bound to His-TAF-Iβ (closed bar), His-TAF-IβPME (gray bar), and His-TAF-I$\beta\Delta$C (open bar) was indicated with bars of SD from triplicate assays.

region of pre-VII in combination with either RRR or the carboxyl-terminal region gains the ability to bind to TAF-I.

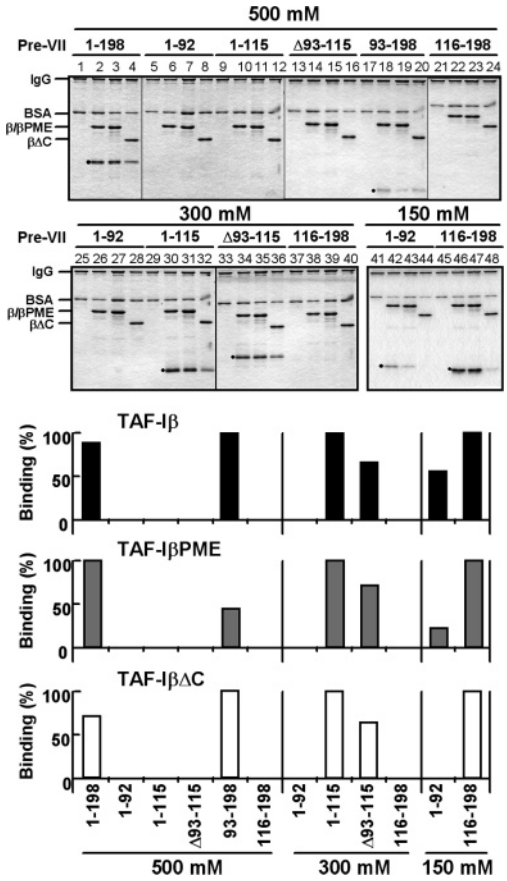

FIGURE 6: Pull-down assays for the TAF-I binding activity of His-pre-VII mutant proteins. His-pre-VII mutant proteins (500 ng) were incubated with 250 ng of His-TAF-Iβ (lanes 2, 6, 10, 14, 18, 22, 26, 30, 34, 38, 42, and 46), His-TAF-IβPME (lanes 3, 7, 11, 15, 19, 23, 27, 31, 35, 43, and 47) or His-TAF-I$\beta\Delta$C (lanes 4, 8, 12, 16, 20, 24, 28, 32, 36, 40, 44, and 48) bound to beads in the presence of 500 mM (lanes 1−24), 300 mM (lanes 25−40), or 150 mM (lanes 41−48) NaCl. Pull-down assays and quantitative measurement were essentially as described in Figure 5C.

Under the same condition, amino-terminal and carboxyl-terminal regions of pre-VII without RRR did not show any TAF-I binding. When examined in the presence of 150 mM NaCl, the carboxyl-terminal region of pre-VII bound to TAF-I more efficiently than the amino-terminal region of pre-VII, supporting the concept that TAF-I preferentially binds to the carboxyl-terminal region of pre-VII.

Binding of Acidic Peptides Derived from TAF-I to RRR of Pre-VII. Next, we tried to determine a region(s) of pre-VII to which the acidic tail of TAF-I binds. To this end, we analyzed the binding efficiency by fluorescence anisotropy assays using a fluorescent probe-labeled acidic peptide which is a part of the acidic tail. The fluorescence anisotropy assay measures the rotational difference between a small molecule labeled with a fluorochrome at a free state and that complexed with another molecule. The small fluorescent probe-labeled molecule rotating randomly at a rapid rate results in rapid light depolarization, while when complexed with a large molecule, it rotates more slowly, and thereby the depolarization rate is reduced. Thus, reduced light depolarization results in anisotropy of the emitted light, which can be measured with polarizer equipment attached to a fluorescence spectrophotometer. The binding efficiency to the acidic peptide was analyzed using various pre-VII mutant proteins. The fluorescent probe-labeled acidic peptide was

Table 1: Acidic Peptide Binding Region of Pre-VII[a]

protein	concn (nM)	protein	concn (nM)
pre-VII(1−198)	16	pre-VII(93−198)	16
pre-VII(1−92)	1065	pre-VII(116−198)	250
pre-VII(1−115)	16	RRR	36
pre-VII(Δ93−115)	53		

[a] Fluorescent probe-labeled acidic peptide (15 nM) was titrated with pre-VII mutant proteins, and the fluorescence anisotropy was measured. The concentrations of pre-VII mutant proteins at 50% of the maximal fluorescence anisotropy are given.

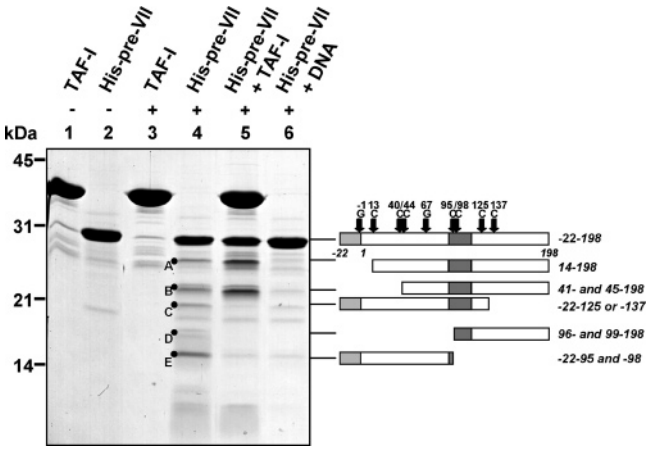

FIGURE 7: Protease sensitivity of His-pre-VII−DNA and His-pre-VII−TAF-I complexes. The DNA−His-pre-VII complex was formed with 1 μg of plasmid DNA and 1.2 μg of His-pre-VII, while the TAF-I−His-pre-VII complex was formed by incubating 3.0 μg of TAF-I with 1.2 μg of His-pre-VII at a molar ratio of 2:1. TAF-I (lane 3), His-pre-VII (lane 4), a mixture of TAF-I and His-pre-VII (lane 5), and a mixture of DNA and His-pre-VII (lane 6) were subjected to partial digestion with α-chymotrypsin. The digestion products were separated by 15% SDS−PAGE and visualized by staining with CBB. Input TAF-I and His-pre-VII are shown in lanes 1 and 2, respectively. The schematic diagram of digestion products corresponding to bands is shown in the right side of the panel.

titrated with pre-VII mutant proteins, and the fluorescence anisotropy was measured. The concentrations of pre-VII mutant proteins at 50% of the maximal fluorescence anisotropy are given in Table 1. The acidic peptide bound to pre-VII mutant proteins, their binding being in the order of RRR > carboxyl-terminal region > amino-terminal region. This order well correlates with the density of the positively charged amino acid in each region (Figure 2A), suggesting that electrostatic effects may determine the strength of the interaction between the acidic peptide and pre-VII.

Protease Sensitivity Assays. The analyses to determine binding regions of each TAF-I and pre-VII had been performed using each deletion mutant protein. Therefore, we tried to examine the binding region again under the condition near the physiological one. Thus, to confirm DNA binding regions and TAF-I binding regions of pre-VII in the presence of physiological ionic strength, we took advantage of protease sensitivity assays (Figure 7). Since protease preferentially attacks a site(s) exposed to the surface of protein and/or protein complexes, a site(s) located at the surface of the protein−protein complex could be identified by partial protease digestion followed by identification of generated fragments. The protease sensitivity assay could be applied to estimate a binding region(s) of a protein of interest complexed with other molecules such that DNase I protection assay is used to identify a recognition site(s) of a sequence-specific DNA binding protein. DNA−His-pre-VII complexes were formed by mixing equal weights of His-pre-VII and plasmid DNA. TAF-I−His-pre-VII complexes were formed by mixing TAF-I and His-pre-VII at a molar ratio of 2:1. In this condition, a dimer of TAF-I binds to a His-pre-VII as already shown by native PAGE (Figure 4). TAF-I (lane 3), His-pre-VII (lane 4), a mixture of TAF-I and His-pre-VII (lane 5), and a mixture of DNA and His-pre-VII (lane 6) were subjected to partial digestion with α-chymotrypsin. TAF-I was not digested by α-chymotrypsin in this condition (lanes 1 and 3). Partial digestion of His-pre-VII gave at least five specific bands, A−E. However, when His-pre-VII was mixed with TAF-I, the intensity of bands A and B increased, whereas that of bands C, D, and E was diminished (lane 5). DNA inhibited digestion of His-pre-VII at all digestion sites of His-pre-VII (lane 6). Bands A−E were identified as described in Experimental Procedures, and possible digestion products of His-pre-VII are indicated in the right side of the panel of Figure 7. These fragments would correspond to bands A−E, respectively, based on their sizes. In addition, bands C and E were confirmed as fragments aa −22−124 or −22−137 and aa −22−95 and −22−98, respectively, since bands C and E were shown to contain the His tag by western blot analyses with anti-polyhistidine antibody. Bands D and E were confirmed as fragments aa 96−198 and 99−198 and aa −22−95 and −22−98, since bands D and E were also generated by digestion of His-pre-VII(93−198) and His-pre-VII(1−115), respectively (data not shown). Endoproteinase Glu-C digested pre-VII at aa 67, and both DNA and TAF-I inhibited digestion at this site (data not shown). Thus, identification of digestion sites reveals that TAF-I efficiently inhibits digestion in the carboxyl-terminal region of His-pre-VII. As noted, the intensity of bands A and B increased when His-pre-VII bound with TAF-I. This could be caused by a conformational change of His-pre-VII induced by binding of TAF-I to the carboxyl-terminal region of His-pre-VII. In conclusion, these results strongly suggested that TAF-I binds to the carboxyl-terminal region of pre-VII containing RRR, while DNA binds equally to the entire pre-VII under a physiological condition.

DISCUSSION

We have characterized the binding mode of pre-VII with DNA and TAF-I. Using pre-VII deletion mutant proteins (Figure 2*A*), we found that RRR of pre-VII dominates in both DNA and TAF-I binding. The amino acid sequence of RRR consists of two basic amino acid clusters of 6 aa and two uncharged amino acids between these two clusters. RRR is also characteristic in protamines, sperm-specific basic proteins. The arginine residues in the DNA binding domain of protamine 1 are present in the center of the molecule in a series of 3−7 arginine clusters connected with one or more uncharged amino acids. Brewer et al. showed that the dissociation constant of such multiple arginine clusters is at least 3 orders of magnitude smaller than that of a single arginine cluster (*31*). The arginine clusters of protamine 1 are predicted to wrap around the major groove of DNA helix and neutralize the negative charge of phosphate groups in the phosphodiester backbone of double-stranded DNA (*32*, *33*). With this assumption, it is likely that RRR of pre-VII

binds to the major groove of DNA. On the basis of UV light-induced cross-linking assays, Chatterjee et al. suggested that RRR binds to the phosphate DNA backbone and α-helices in the carboxyl-terminal portion of protein VII dock with the major groove of DNA (*25*).

In addition to RRR, amino-terminal and carboxyl-terminal regions of pre-VII were shown to have potential to bind DNA directly. These regions showed stronger DNA binding activity with RRR than each region alone. The DNA binding activity of both regions was sensitive to increasing concentrations of NaCl (Figure 3). This result suggests that ionic interaction rather than hydrogen bonding is dominant for DNA binding. The ionic interaction between the acidic tail of TAF-I and pre-VII was also suggested by fluorescence anisotropy measurements (Table 1). These results lead to the assumption that DNA and the acidic tail of TAF-I compete with each other to bind to pre-VII. By the fluorescence anisotropy competition assay where pre-VII−acidic peptide complexes were titrated with DNA, DNA was found to replace the probe-labeled acidic peptide more efficiently than the cold acidic peptide (data not shown). Recently, Lee et al. (*34*) proposed a DNA binding region of pre-VII by examining chromosome localization of a pre-VII fragment fused to GFP in mitotic cells. They reported that GFP-fused peptides of aa 25−54 and aa 134−198 of pre-VII are associated to the mitotic chromosome and suggested that these regions alone are sufficient for retention on DNA. This is in good agreement with results of our protease sensitivity assay showing that every digestion site of pre-VII was protected by DNA. Since the region between aa 25−54 contains the high density of basic amino acids, it is reasonable that pre-VII(1−92) and pre-VII(116−198) used in this study containing the highly basic regions of aa 25−54 and aa 134−198, respectively, are capable of binding to DNA as shown in the nitrocellulose filter binding assay (Figure 3).

Pull-down assays (Figure 6) showed that a mutant pre-VII comprising RRR and the carboxyl-terminal region is a strong binder for TAF-IβΔC as well as TAF-Iβ. Protease sensitivity assays showed that the amino-terminal region (aa 1−40) of pre-VII is accessible for α-chymotrypsin, even when complexed with TAF-I. The region between aa 94−148 of protein VII (aa 118−172 of pre-VII) fused to GST was shown to bind to TAF-I in cell extracts by Xue et al. (*10*). Taken altogether, it is quite likely that the major TAF-I binding region consists of the carboxyl-terminal region and RRR.

TAF-I monomer mutants and TAF-I mutants lacking the acidic tail are not capable of remodeling the Ad core. Pull-down assays showed that a TAF-I monomer mutant binds to protein VII with 2-fold less efficiency than the full-length TAF-I, and a TAF-I mutant lacking the acidic tail binds to protein VII with almost similar efficiency of the full-length TAF-I in the presence of 500 mM NaCl. These results suggest that the amino-terminal region of TAF-I, irrespective of its involvement in dimerization, binds to protein VII. The hydrophilic surface of the coiled-coil region is predicted to be rich in aspartic and glutamic acids (*19*), so it is possible that the hydrophilic surface of the coiled-coil region is directly involved in pre-VII and protein VII binding. We speculate that the region of TAF-I except for the acidic tail determines the specificity in binding with protein VII, and a

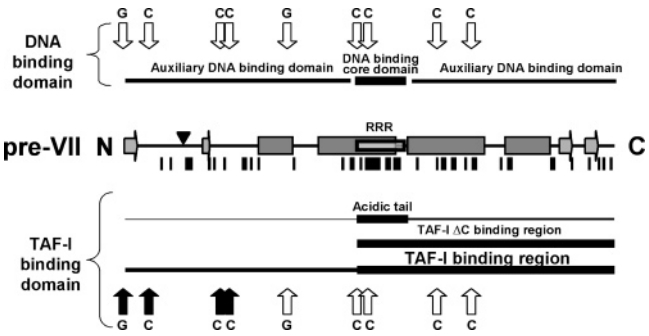

FIGURE 8: Summary of the present study. The major interaction between pre-VII and DNA or TAF-Iβ is mediated through the positively charged RRR of pre-VII (the thicker the line, the stronger the binding). The amino-terminal and carboxyl-terminal regions of pre-VII enhance the DNA binding activity of pre-VII by direct DNA interaction. TAF-I lacking the acidic tail preferentially binds to the carboxyl-terminal region of pre-VII containing RRR. Vertical closed and open arrows indicate protease digestion sites, where digestion is sensitive or insensitive, respectively, when complexed with DNA and TAF-I (C and G indicate chymotrypsin and Glu-C, respectively). The secondary structure predicted by HNN (Guermeur thesis, 1997) is depicted with gray rectangles for α-helix and horizontal arrows for β-sheet. Arginine and lysine are indicated by vertical bars. The arrowhead indicates the cleavage site by adenovirus protease.

pair of the acidic tails in a dimer of TAF-I contributes to the binding by their nonspecific ionic interaction. This prediction about a role of acidic clusters could be generalized for acidic histone chaperones containing acidic clusters. An acidic cluster of NAP-1 is dispensable for nucleosome assembly in vitro but contributes to binding of NAP-1 to histones through structure-independent electrostatic interactions (*35*, *36*). Removal of the acidic tail of nucleoplasmin does not alter the binding property of nucleoplasmin with histones (*37*). The acidic tail of nucleoplasmin, while enhancing the efficiency of protamine removal, is dispensable for sperm chromatin decondensation in vitro (*38*, *39*). In the previous report (*18*), we assumed the structure of protein VII−TAF-I complexes in the presence of an excess amount of TAF-I in such a way that each acidic tail in a TAF-I dimer interacts with each one of two basic regions of protein VII. From this study, the previous model could be revised as that one TAF-I dimer lacking the acidic tail binds to one carboxyl-terminal region containing RRR of protein VII and each one of the acidic tails may also bind to RRR and the carboxyl-terminal region of protein VII.

The present study indicates that DNA binding regions and TAF-I binding regions of pre-VII are partially overlapping (Figure 8). The amino-terminal region of pre-VII is free from TAF-I in the TAF-I−pre-VII complex (Figure 7). Thus, we would propose the mechanism of remodeling of the DNA−protein VII complex by TAF-I as follows: a TAF-I dimer binds to protein VII through the carboxyl-terminal region containing RRR in DNA−protein VII complexes. TAF-I dissociates the carboxyl-terminal region of protein VII from DNA, while the amino-terminal region of protein VII remains bound to DNA. By the formation of this ternary complex, DNA−protein VII interaction would be reduced because of loss of the carboxyl-terminal region-mediated DNA binding.

Although we showed that pre-VII binds to DNA or TAF-I in almost the same manner as protein VII in the binary complex formation, we cannot exclude the possibility that pre-VII and protein VII differ from each other when they

are complexed with negatively charged molecules. Some different properties in terms of the DNA binding are found between protein VII and pre-VII (*21*, *24*). Of interest is that TAF-I binds to DNA−protein VII complexes forming a ternary complex, while TAF-I dissociates pre-VII from DNA−pre-VII complexes (unpublished observation). Pre-VII−TAF-I and pre-VII−DNA complexes are present in infected cells in late phases of infection (Figure 1). Experiments are ongoing to understand the molecular mechanism of complex conversion from pre-VII−TAF-I and pre-VII−DNA, the latter of which is to be packed in virions.

ACKNOWLEDGMENT

We thank Dr. Weber for providing us with human Ad type 2 ts1, Dr. Shimizu for MS analysis, and Dr. Okuwaki for careful reading of the manuscript and useful comments.

REFERENCES

1. de la Cruz, X., Lois, S., Sanchez-Molina, S., and Martinez-Balbas, M. A. (2005) Do protein motifs read the histone code?, *BioEssays 27*, 164−175.
2. Lusser, A., and Kadonaga, J. T. (2003) Chromatin remodeling by ATP-dependent molecular machines, *BioEssays 25*, 1192−200.
3. Loyola, A., and Almouzni, G. (2004) Histone chaperones, a supporting role in the limelight, *Biochim. Biophys. Acta 1677*, 3−11.
4. Ohsumi, K., and Katagiri, C. (1991) Characterization of the ooplasmic factor inducing decondensation of and protamine removal from toad sperm nuclei: involvement of nucleoplasmin, *Dev. Biol. 148*, 295−305.
5. Philpott, A., Leno, G. H., and Laskey, R. A. (1991) Sperm decondensation in Xenopus egg cytoplasm is mediated by nucleoplasmin, *Cell 65*, 569−578.
6. Matsumoto, K., Nagata, K., Miyaji-Yamaguchi, M., Kikuchi, A., and Tsujimoto, M. (1999) Sperm chromatin decondensation by template activating factor I through direct interaction with basic proteins, *Mol. Cell. Biol. 19*, 6940−6952.
7. Chatterjee, P. K., Vayda, M. E., and Flint, S. J. (1985) Interactions among the three adenovirus core proteins, *J. Virol. 55*, 379−386.
8. Chatterjee, P. K., Vayda, M. E., and Flint, S. J. (1986) Adenoviral protein VII packages intracellular viral DNA throughout the early phase of infection, *EMBO J. 5*, 1633−1644.
9. Spector, D. J., Johnson, J. S., Baird, N. L., and Engel, D. A. (2003) Adenovirus type 5 DNA-protein complexes from formaldehyde cross-linked cells early after infection, *Virology 312*, 204−212.
10. Xue, Y., Johnson, J. S., Ornelles, D. A., Lieberman, J., and Engel, D. A. (2005) Adenovirus protein VII functions throughout early phase and interacts with cellular proteins SET and pp32, *J. Virol. 79*, 2474−2483.
11. Matsumoto, K., Nagata, K., Ui, M., and Hanaoka, F. (1993) Template activating factor I, a novel host factor required to stimulate the adenovirus core DNA replication, *J. Biol. Chem. 268*, 10582−10587.
12. Matsumoto, K., Okuwaki, M., Kawase, H., Handa, H., Hanaoka, F., and Nagata, K. (1995) Stimulation of DNA transcription by the replication factor from the adenovirus genome in a chromatin-like structure, *J. Biol. Chem. 270*, 9645−9650.
13. Nagata, K., Kawase, H., Handa, H., Yano, K., Yamasaki, M., Ishimi, Y., Okuda, A., Kikuchi, A., and Matsumoto, K. (1995) Replication factor encoded by a putative oncogene, set, associated with myeloid leukemogenesis, *Proc. Natl. Acad. Sci. U.S.A. 92*, 4279−4283.
14. Okuwaki, M., and Nagata, K. (1998) Template activating factor-I remodels the chromatin structure and stimulates transcription from the chromatin template, *J. Biol. Chem. 273*, 34511−34518.
15. Kawase, H., Okuwaki, M., Miyaji, M., Ohba, R., Handa, H., Ishimi, Y., Fujii-Nakata, T., Kikuchi, A., and Nagata, K. (1996) NAP-I is a functional homologue of TAF-I that is required for replication and transcription of the adenovirus genome in a chromatin-like structure, *Genes Cells 1*, 1045−1056.
16. Okuwaki, M., Iwamatsu, A., Tsujimoto, M., and Nagata, K. (2001) Identification of nucleophosmin/B23, an acidic nucleolar protein, as a stimulatory factor for in vitro replication of adenovirus DNA complexed with viral basic core proteins, *J. Mol. Biol. 311*, 41−55.
17. Okuwaki, M., Matsumoto, K., Tsujimoto, M., and Nagata, K. (2001) Function of nucleophosmin/B23, a nucleolar acidic protein, as a histone chaperone, *FEBS Lett. 506*, 272−276.
18. Haruki, H., Gyurcsik, B., Okuwaki, M., and Nagata, K. (2003) Ternary complex formation between DNA-adenovirus core protein VII and TAF-Ibeta/SET, an acidic molecular chaperone, *FEBS Lett. 555*, 521−527.
19. Miyaji-Yamaguchi, M., Okuwaki, M., and Nagata, K. (1999) Coiled-coil structure-mediated dimerization of template activating factor-I is critical for its chromatin remodeling activity, *J. Mol. Biol. 290*, 547−557.
20. Black, B. C., and Center, M. S. (1979) DNA-binding properties of the major core protein of adenovirus 2, *Nucleic Acids Res. 6*, 2339−2353.
21. Sato, K., and Hosokawa, K. (1984) Analysis of the interaction between DNA and major core protein in adenovirus chromatin by circular dichroism and ultraviolet light induced cross-linking, *J. Biochem. (Tokyo) 95*, 1031−1039.
22. Weber, J. (1976) Genetic analysis of adenovirus type 2 III. Temperature sensitivity of processing viral proteins, *J. Virol. 17*, 462−471.
23. Cai, F., and Weber, J. M. (1993) Primary structure of the canine adenovirus PVII protein: functional implications, *Virology 193*, 986−988.
24. Chatterjee, P. K., Yang, U. C., and Flint, S. J. (1986) Comparison of the interactions of the adenovirus type 2 major core protein and its precursor with DNA, *Nucleic Acids Res. 14*, 2721−2735.
25. Chatterjee, P. K., Vayda, M. E., and Flint, S. J. (1986) Identification of proteins and protein domains that contact DNA within adenovirus nucleoprotein cores by ultraviolet light cross-linking of oligonucleotides ^{32}P-labelled in vivo, *J. Mol. Biol. 188*, 23−37.
26. Nagata, K., Saito, S., Okuwaki, M., Kawase, H., Furuya, A., Kusano, A., Hanai, N., Okuda, A., and Kikuchi, A. (1998) Cellular localization and expression of template-activating factor I in different cell types, *Exp. Cell Res. 240*, 274−281.
27. Gill, S. C., and von Hippel, P. H. (1989) Calculation of protein extinction coefficients from amino acid sequence data, *Anal. Biochem. 182*, 319−326.
28. Kaiser, E., Colescott, R. L., Bossinger, C. D., and Cook, P. I. (1970) Color test for detection of free terminal amino groups in the solid-phase synthesis of peptides, *Anal. Biochem 34*, 595−598.
29. Wu, J., and Filutowicz, M. (1999) Hexahistidine (His6)-tag dependent protein dimerization: a cautionary tale, *Acta Biochim. Pol. 46*, 591−599.
30. Hang, Q., Woods, L., Feiss, M., and Catalano, C. E. (1999) Cloning, expression, and biochemical characterization of hexahistidine-tagged terminase proteins, *J. Biol. Chem. 274*, 15305−15314.
31. Brewer, L., Corzett, M., Lau, E. Y., and Balhorn, R. (2003) Dynamics of protamine 1 binding to single DNA molecules, *J. Biol. Chem. 278*, 42403−42408.
32. Fita, I., Campos, J. L., Puigjaner, L. C., and Subirana, J. A. (1983) X-ray diffraction study of DNA complexes with arginine peptides and their relation to nucleoprotamine structure, *J. Mol. Biol. 167*, 157−177.
33. Prieto, M. C., Maki, A. H., and Balhorn, R. (1997) Analysis of DNA-protamine interactions by optical detection of magnetic resonance, *Biochemistry 36*, 11944−11951.
34. Lee, T. W., Blair, G. E., and Matthews, D. A. (2003) Adenovirus core protein VII contains distinct sequences that mediate targeting to the nucleus and nucleolus, and colocalization with human chromosomes, *J. Gen. Virol. 84*, 3423−3428.
35. Fujii-Nakata, T., Ishimi, Y., Okuda, A., and Kikuchi, A. (1992) Functional analysis of nucleosome assembly protein, NAP-1. The negatively charged COOH-terminal region is not necessary for the intrinsic assembly activity, *J. Biol. Chem. 267*, 20980−20986.
36. McBryant, S. J., Park, Y. J., Abernathy, S. M., Laybourn, P. J., Nyborg, J. K., and Luger, K. (2003) Preferential binding of the histone $(H3-H4)_2$ tetramer by NAP1 is mediated by the amino-terminal histone tails, *J. Biol. Chem. 278*, 44574−44583.

37. Arnan, C., Saperas, N., Prieto, C., Chiva, M., and Ausio, J. (2003) Interaction of nucleoplasmin with core histones, *J. Biol. Chem. 278*, 31319−31324.
38. Prieto, C., Saperas, N., Arnan, C., Hills, M. H., Wang, X., Chiva, M., Aligue, R., Subirana, J. A., and Ausio, J. (2002) Nucleoplasmin interaction with protamines. Involvement of the polyglutamic tract, *Biochemistry 41*, 7802−7810.
39. Banuelos, S., Hierro, A., Arizmendi, J. M., Montoya, G., Prado, A., and Muga, A. (2003) Activation mechanism of the nuclear chaperone nucleoplasmin: role of the core domain, *J. Mol. Biol. 334*, 585−593.

BI051248+